John von Neumann Institute for Computing

Entangled Polymers: From Universal Aspects to Structure Property Relations

Kurt Kremer

published in

Computational Soft Matter: From Synthetic Polymers to Proteins, Lecture Notes,
Norbert Attig, Kurt Binder, Helmut Grubmüller, Kurt Kremer (Eds.),
John von Neumann Institute for Computing, Jülich,
NIC Series, Vol. **23***, ISBN 3-00-012641-4, pp. 141-168, 2004.*

© 2004 by John von Neumann Institute for Computing
Permission to make digital or hard copies of portions of this work for personal or classroom use is granted provided that the copies are not made or distributed for profit or commercial advantage and that copies bear this notice and the full citation on the first page. To copy otherwise requires prior specific permission by the publisher mentioned above.

http://www.fz-juelich.de/nic-series/volume23

Entangled Polymers: From Universal Aspects to Structure Property Relations

Kurt Kremer

Max-Planck-Institut für Polymerforschung,
55021 Mainz, Germany
E-mail: kremer@mpip-mainz.mpg.de

Simulations are very versatile tools to study the relaxations and dynamics of polymer melts and networks. The fact that polymer chains cannot pass through each other poses special difficulties for analytic theories, while on the other hand many experiments are dominated by this fact. The paper discusses some basic concepts and conditions and ways to study such problems by computer simulations.

1 Introduction

In the previous lectures of this school the basic concepts to describe polymer melts or dense solutions were introduced and discussed (cf. chapters by J. Baschnagel et al, B. Dünweg and W. Paul). Among others random walks, excluded volume screening, the Rouse model as well as the reptation concept have been included. In the present chapter I mainly focus on the consequences of the fact that chains cannot pass through but only along each other, which eventually leads to the reptation or tube model. To discuss this I will shortly review the background coming from the Rouse model and then discuss similarities between polymer melts and networks, as they are observed experimentally and as they can be studied in different details in a simulation. Since most of the information gained by simulation is complementary to typical (scattering) experiments an altogether rather coherent picture has emerged over the many years of research[1–3].

Dense polymer systems such as melts, glasses, and crosslinked melts or solutions (networks such as rubber and gels) are very complex materials. Besides the local chemical interactions and density correlations, which are common to all disordered liquids and solids the global chain conformations and the chain connectivity play a decisive role for many physical properties. Local interactions determine the liquid structure on the scale of a few $\AA$ or at most a few nm. This question has been examined in detail by the contribution of W. Paul, where simulations of atomistically detailed melts are discussed. When we look at the dynamics of a polymer chain in such a melt local interactions determine the packing and the bead friction but not the generic properties[4]. It is the main focus of the present contribution to discuss generic aspects common to all polymers and then lateron go back to the question to what extent chemistry specific aspects play a role or make a difference. The consequences of the latter are also termed as structure property relations (SPR) in applied research[5,6].

To stick to simple situations we consider polymer melts or networks where the chains are all identical. They can be characterized by an overall particle density ρ and a number of monomers N per chain. As shown in previous chapters, the overall extension of the chains is well characterized by the properties of random walks[7–9]. With ℓ being the average bond length we then have (for $N >> 1$) for the mean square end to end distance

$$\langle R^2(N)\rangle = \ell_K \ell (N - I) \approx \ell_K \ell N \tag{1}$$

and $\langle R_G^2(N)\rangle = \frac{1}{6}\langle R^2(N)\rangle$ for the radius of gyration respectively. ℓ_K is the Kuhn length and a measure for the stiffness of the chain. This gives an average volume per chain of

$$V \propto \langle R^2(N)\rangle^{3/2} \sim N^{3/2} \tag{2}$$

leading to a vanishing self density of the chains in a melt. In order to pack beads to the monomer density ρ, $0(N^{1/2})$ other chains share the volume of the very same chain. These other chains effectively screen the long range excluded volume interaction, since the individual monomer cannot distinguish, whether a non-bonded neighbor monomer belongs to the same chain or not. This general property is firmly established by experiment and many simulations[10].

On very large scales polymers diffuse as a whole and the motion is well described by standard diffusion. However over distances up to the order of the chain size, the motion of a polymer chain is more complex, even though hydrodynamic interactions are screened and do not play a role. A detailed discussion of hydrodynamic effects is given by B. Dünweg in this school. The random motion of a monomer is constrained by the chain connectivity and the interaction with other monomers. To a very good first approximation, the other chains can be viewed as providing a viscous background and a heat bath. This certainly is a drastic oversimplification, which ignores all correlations due to the structure of the surrounding. The advantage of this simplification is that the Langevin dynamics of a single chain of point masses connected by harmonic springs can be solved exactly[1]. This was first done in a seminal paper by Rouse[11] and about the same time in a similar fashion by Bueche[12]. In this model, which is commonly referred to as the Rouse model, the diffusion constant of the chain $D \sim N^{-1}$, the longest relaxation time $\tau_d \sim N^2$ and the viscosity $\eta \sim N$. This describes the dynamics of a melt of relatively short chains, meaning e.g. $M \leq 20\,000$ for polystyrene [PS] or $M \leq 2000$ for polyethylene [PE], both qualitatively and quantitatively almost perfectly, though the reason is not well understood. Only recently some deviations have been observed[13]. The effects are rather subtle and would require a detailed discussion beyond the scope of this lecture. For longer chains, the motion of the chains are observed to be significantly slower. Experiments show a dramatic decrease in the diffusion constant, $D \sim N^{-2.414}$, and an increase in the viscosity towards $\eta \sim N^{3.41}$. The time-dependent modulus $G(t)$ exhibits a solid or rubber-like plateau at intermediate times before decaying completely. Since the properties for all systems start to change in the same way at a chemistry- and temperature-dependent chain length N_e or molecular weight M_e, one is led to the idea that this can only originate from properties common to all chains, namely the chain connectivity and the fact that the chains cannot pass through each other. This is what I am going to discuss in the subsequent chapters.

2 Polymer Dynamics and Network Elasticity

The plateau modulus $G(t)$ can be derived from the restoring force of a polymer melt or network after a step strain. Experimentally usually an oscillatory shear is applied. What one finds then is illustrated in Fig. (1).

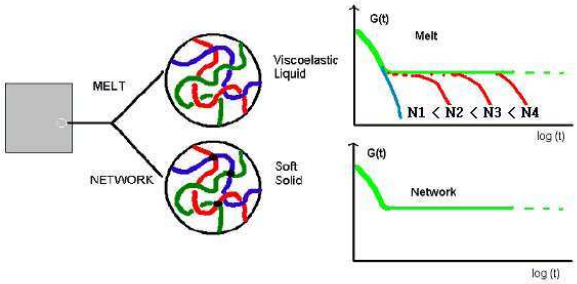

Figure 1. Cartoon of the characteristic structure and response of a polymer melt (top) and a polymer network (bottom) after a step strain. For short chains (length N1) the restoring force decays to zero very fast, while for the longer ones with increasing length N, as indicated, a plateau in the time dependent modulus occurs, which is independent N

After a drastic fast initial decay, if the chains are long enough, the modulus $G(t)$ stays almost constant at a value G_N^o for a long time until $G(t)$ eventually decays to zero. Many related experimental findings can be found in Ferry's book from 1980[15]. Fig. (1) illustrates the similarities between cross-linked melts (rubber) and non-cross-linked melts. In both cases the value of the plateau modulus eventually becomes independent of N, which is either the chain length of the melt or the average strand length between two cross-links, if only N is large enough. These similarities lead to the famous reptation or tube concept by Edwards[16] and deGennes[17].

Edwards in his work on cross-linked networks introduced the concept of obstacles created by the other chains, resulting in a "tube" in which the monomers move. Fig. (2) shows a "historical" sketch of the development of this concept. First consider a network. The figure shows one strand of the network in the center marked by a thick line and a rather crude sketch of the surrounding. Edwards discussed how the black center chain could move around subject to obstacles created by all the other chains which in this case are part of the network. He noted that due to the topological constraints the chain is much more localized than expected just by the fact that the two ends are connected to a cross-link. All loops and their links in the system are conserved; they cause the strand to be essentially confined to a tube-like region (Fig. (2), middle part). This hypothetical tube, built by all the other chains, follows the coarse-grained conformation of the chain. The length scale of this coarse graining is called the entanglement length N_e and a sphere of the diameter d_T of the tube typically contains $d_T^{1/\nu} = N_e$ monomers, where ν = 1/2 is the random walk exponent. Within this picture the strand can perform a quasi one-dimensional Rouse relaxation along that tube. Later, deGennes realized that the motion and spatial fluctuations of long chains in melts should be governed by the same mechanism (Fig. (2), lower part). When the chains are very long, most of the monomers are far from the chain end. Then, on intermediate time scales, these monomers do not realize that the ends are free. Since the density of chain ends is very small, $O(\rho/N)$, the topology of the surrounding does not change significantly on these intermediate time scales and a chain can only diffuse by reptating out of its original tube. This gives $D \sim N^{-2}, \tau_d \sim N^3$ as well as a plateau modulus at intermediate time scales. Considering the simplicity of the concept, the model describes many experimental findings remarkably well. However, in spite of its successes,

several open questions remain, including how to formulate the reptation concept on a more fundamental basis.

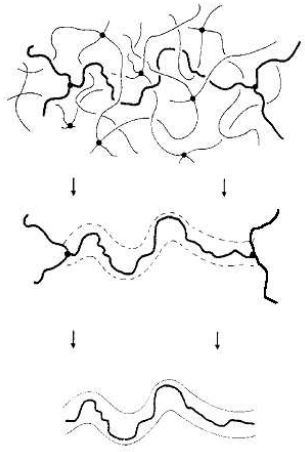

Figure 2. Sketch of the historical development of the tube constraint and reptation concept. Starting from a network Edwards in 1967 defined the confinement to the tube, while deGennes in 1971 realized that for long chains the ends only play a small role for intermediate times.

A quantitative structure based model or theory of what an entanglement really is, remained largely unsettled until some very recent progress[18–20]. Also the discrepancy between the observed viscosity of $\eta \propto N^{3.4}$ and the predicted power law $\eta \propto N^3$ by now is safely attributed to a very slow crossover towards the asymptotic regime[2]. This is a little different for the diffusion of constant D, where the most complete and careful collection of data finds $D \propto N^{-2.4}$ instead of N^{-2}. Here it is not yet settled whether this is the "same" crossover effect[21] or whether this is mostly due to the so called correlation hole[a] effect. A detailed discussion however is beyond the scope of the present contribution.

There have also been a variety of nonreptation/tube phenomenological approaches, which only treat the interactions between the chains either in an averaged mean field approximation or develop a memory function formalism. Though they can reproduce experimental data to some degree, they fail when it comes to the microscopic motions of the polymers and the confinement due to the surrounding strands. Here I do not discuss these approaches any further. Rather comprehensive reviews are given by McLeish[2] and on the simulation aspects by Kremer and Grest[3](and references therein). In a similar way our understanding of networks has improved over the last years. It has been known for a long time, especially also due to simulations, that the noncrossability of the chains plays an important role for the elasticity and related phenomena. Experiments on networks with the

[a]The correlation hole is defined by the self density of the chain in the melt. The density $\rho = \rho(r)_{other} + \rho_{self}(r)$ with $\rho_{self} \simeq N/R^3 \propto N^{-1/2}$. Viewing the chains as very soft spheres these spheres like in a liquid of ordinary spheres have to leave their cage when diffusing around. This leads to a back jump correlation and slows down the diffusion beyond the influence of the microscopic bead friction. Note that the center of gravity of a chain not necessarily has to move in order to relax the overall chain conformation.

same average strand length but cross-linked at different initial concentrations directly prove this point. However, when it comes to the question of identifying the different contributions (cross-links and entanglements) still conceptual problems exist. Also, the comparison of scattering experiments to theory/simulation only very recently made some significant progress. There the relaxation phenomena are only partially the same as for melts, since the cross-links at the chain ends introduce boundary conditions for the tube contour which do not exist for uncross-linked melts[22,23].

From the above it is clear that computer simulations can be a very versatile tool to investigate such problems, since they offer the unique opportunity to have full control over the chain conformations while simultaneously typical experimental observables can be "measured". Though CPU time intensive, simulations have played an important role over the years and will continue to do so.

Experimental quantities such as the viscosity, diffusion constant and modulus do not directly probe the microscopic motion of monomers on the chain. In contrast neutron spin-echo scattering covers the appropriate length scales, but the time range is rather limited. Pulsed large field gradient spin-echo NMR is able to address the appropriate time and distance scales as well. However, an experiment typically probes one aspect only. Also samples are never really ideal and one must e.g. deal with polydispersity effects. Simulations do not suffer from such problems and can now be performed on melts of chains of 15 - 20 N_e, answering a number of unsolved questions.

3 Theoretical Concepts

The Rouse and reptation models are also shortly discussed in the contributions by W. Paul, J. Baschnagel, and B. Dünweg. I now first review some more of the background, restricting myself mostly to quantities which can be investigated directly by simulation. In a melt of homopolymers, the excluded volume interaction is effectively screened. There is no tendency for a chain to swell beyond the ideal random-walk dimension. Only the prefactor, or more precisely the Kuhn length l_K ($\ell_K = \ell c_\infty$ in Flory's terminology[24]), is governed by the local monomer-monomer interactions.

3.1 Unentangled Chains - Rouse Regime

In the Rouse model, all the complicated interactions are absorbed into a monomeric friction and a coupling to a heat bath. It was originally proposed to model an isolated chain in solution, though it actually works very well for short chains in a melt. For chains in solution we refer to the chapter by Dünweg in this volume. Here I follow essentially the book of Doi and Edwards[1] and a recent review by McLeish[2]. The polymer is modelled as a freely jointed chain of N beads connected by N - 1 springs, immersed in a Newtonian continuum. Hydrodynamic interactions are neglected. Each bead experiences a friction, with friction coefficient ζ. The beads are connected by a Hookean spring with a force constant $k = 3k_BT/b^2$, where $b^2 = \ell\ell_K$. Each bead-spring unit is intended to model a subchain of the real molecule, not a monomer. The equation of motion of the beads is given by a Langevin equation. For monomer $i (i \neq 1, N)$ it reads,

$$\zeta \dot{\mathbf{r}}_i = k(2\mathbf{r}_i - \mathbf{r}_{i-1} - \mathbf{r}_{i+1}) + \mathbf{f}_i \tag{3}$$

Usually the model is solved for a ring with no free ends. If the chain ends are free, as for all linear chains, the first and the last monomer have to be treated differently. For i = 1, the first term on the right hand side is $-k(\mathbf{r}_1 - \mathbf{r}_2)$ and similarly for $i = N$. The distribution of random forces $\mathbf{f}_i$ is Gaussian with zero mean and the second moment:

$$\langle \mathbf{f}_i(t) \cdot \mathbf{f}_j(t') \rangle = 6\zeta k_B T \delta_{ij} \delta(t - t'). \tag{4}$$

Note that this model does not contain any specific interactions between monomers except those due to the chain connectivity. Since in a melt, the long-range hydrodynamic interactions are screened, it was suggested that this model could describe the motion of those chains, except that ζ arises from other chains rather than the solvent.

The Rouse model can be solved by transforming to normal coordinates $\mathbf{X}_p(t)$ of the chain. For a discrete monomer chain these are given by[5]

$$\mathbf{X}_p(t) = \frac{1}{N-1} \sum_{i=1}^{N-1} \mathbf{r}_i(t) cos \frac{p\pi(i+1/2)}{N-1} \tag{5}$$

and $p = 0, 1, 2, \ldots, N$ - 1. Equation (3) can be rewritten as

$$\zeta_p \dot{\mathbf{X}}_p = k_p \mathbf{X}_p + \mathbf{f}_p \tag{6}$$

where $\zeta_0 = N\zeta$ and $\zeta_p = 2N\zeta$ for $p \geq 1$ and

$$k_p = 8Nksin^2 \frac{p\pi}{2(N-1)}. \tag{7}$$

For small p/N, one recovers the usual result

$$k_p = 2\pi^2 k_p^2/N = \frac{6\pi^2 k_B T}{N\ell\ell_K} p^2 \tag{8}$$

with $Nb^2 = \langle R^2 \rangle$. Since the random forces $\mathbf{f}_p$ are not correlated, the $\mathbf{X}_p$ decouple and the motion of the polymer can be decomposed into independent modes.

For chains in a melt, the Rouse modes are eigenmodes of the chains. This has been verified by MD for melts of short chains. The time correlation functions of the normal modes, $p \geq 1$, are

$$R_p(t) = \frac{< \mathbf{X}_p(t) \cdot \mathbf{X}_p(0) >}{< X_p^2(0) >} = exp(-t/\tau_p), \;\; \tau_p = \frac{\zeta(\ell\ell_K)^2 NN}{3\pi^2 k_B T p^2}, \tag{9}$$

where we have used the small p/N approximation for k_p. The longest relaxation time is $\tau_R = \tau_1 \sim N^2$. For long chains in a melt, this equation is expected to only describe the relaxation of high p modes with $N/p \leq N_e$. The relaxation modulus of the melt is given by

$$G(t) = \frac{\rho k_b T}{N} \sum_p R_p(2t). \tag{10}$$

where ρ is the monomer density. This assumes that the single chain Rouse modes can be taken as eigenmodes of the whole melt. This certainly is an assumption, as briefly discussed in the introduction. For the Rouse model this gives

$$G(t) = \frac{pK_BT}{N} \sum_P exp(-2tp^2/\tau_R) \tag{11}$$

and the viscosity η reads

$$\eta = \int_0^\infty G(t)dt = \frac{\rho k_BT}{2N} \sum_p \tau_p = \frac{\pi^2 \rho k_BT}{12N} \tau_R = \frac{\rho\zeta}{36} < R^2 > \sim N\zeta \tag{12}$$

The self-diffusion constant D can be determined from the mean-square displacement of $\mathbf{X}_0 = \mathbf{r}_{cm}$, the center-of mass of the chain,

$$g_3(t) =< (\mathbf{r}_{cm}(t) - \mathbf{r}_{cm}(0))^2 > \tag{13}$$

Within the Rouse model $g_3(t) \sim t$ for all times and the diffusion constant $D(N) = lim_{t\to\infty} g_3(t)/6t$ is expected to reach the asymptotic value

$$D = \frac{k_BT}{N\zeta} \tag{14}$$

for relatively short times. In simulations often the mean-square displacement of a monomer $g_1(t)$ as a function of time t

$$g_1(t) = \frac{1}{N} \sum_i^N = 1\langle[\mathbf{r}_i(t) - \mathbf{r}_i(0)]^2\rangle. \tag{15}$$

is studied. Using the fact that the chain structure is that of a random walk, it is easy to show that

$$g_1(t) \sim \begin{cases} t^1, & t < \tau_0, \quad g_1(t) < \ell\ell_K \\ t^{1/2}, & \tau_0 < t < \tau_R, \; g_1(t) \lesssim \langle R^2\rangle \\ t^1, & t > \tau_R, \quad g_1(t) \gtrsim \langle R^2\rangle \end{cases} \tag{16}$$

For very short times, when a monomer has moved less than its own diameter, it is affected little by its neighbors along the chain. This short time regime, $t < \tau_0$ is governed by the local chemical/model properties of the chains. Within the worm-like chain model in which the chain is a continuous flexible path, τ_0 is zero. For intermediate times, the motion of a monomer is slowed down because it is connected to other monomers. This can be viewed as the diffusion of a particle with increasing distance dependent mass. The actual mass at time t is just the number of monomers within a sphere of diameter $\sqrt{g_1(t)}$. This continues until the chain has moved a distance comparable to its size $\langle R^2\rangle^{1/2}$. After that is observed free diffusion with a diffusion coefficient $D \sim N^{-1}$. It turns out experimentally that this extremely simple model provides an excellent description of polymer dynamics, provided that the chains are short enough. Measurements of η[15] as well as NMR[25,26]and

neutron spin-echo scattering experiments[27] which probe the motion of the monomers agree to that. Results for molecular dynamics simulations on short chains also agree surprisingly well. For short chains, it turns out that the noncrossability of the chains, as well as the chain nature and chemical structure of the surrounding of each monomer mostly affects the prefactors in the diffusion coefficient through the monomeric friction coefficient ζ. Why these effects average to such a simple contribution still is not understood.

3.2 Entangled Chains

For chains which significantly exceed the length N_e, the motion is slowed down drastically. Clearest evidence for this slowing down comes from the diffusion constant D[14,28,29]. For $N \geq N_e$,

$$D \sim N^{-2} \ldots N^{-2.4} \tag{17}$$

Several forms for the prefactor of D have been discussed in the literature. Similarly the viscosity η increases so that

$$\eta \sim N^{3.4} \tag{18}$$

compared to N for short chains. In the reptation theory the motion of the chains is viewed as Rouse motion of chains in a tube of diameter d_T, which follows the coarse grained back bone of the chain. Since the chain is modelled as a random walk, forces at the ends have to keep a tube contour length $L_T \sim N$. In the original concept the tube is fixed and the chain had to completely move out of the tube to relax its conformation and any stress linked to the conformation. All other means of relaxation, such as constraint release due to chain ends or fluctuation effects like contour length fluctuations of the tube modify this scheme only somewhat quantitatively, but do not alter the qualitative picture. I thus will here discuss the simplest case only[1].

For short time scales the motion of the monomers cannot be distinguished from that of the Rouse model, the motion of the monomer is isotropic and $g_1(t) \sim t^{1/2}$. Only after the motion reaches a distance of the $O(d_T^2 \equiv \langle R^2(N_e)\rangle)$ the constraints from the tube are showing up. The corresponding time is the Rouse time of a subchain of N_e beads, namely $\tau_e \sim N_e^2$. After this time the monomers can diffuse along the tube only. By this forward and backward motion, the chain explores new space and slowly destroys the original tube. The contour length of the tube L_T can be estimated to $L_T \approx d_T N/N_e \sim N/N_e^{1/2}$. For $t > \tau_e$, the chain performs essentially a one dimensional Rouse motion along the random walk like tube turning the $t^{1/2}$ power law for $g_1(t)$ into a $t^{1/4}$ power law. However, after the Rouse relaxation time τ_R, the monomers have only moved a distance of order $L_T^{1/2} \ll L_T$ for $N \gg N_e$. Following this regime the overall diffusion along the tube gives a second $t^{1/2}$ regime for the motion in space. There the elemental step is the displacement of a polymer chain along its tube. The longest relaxation time is the mean lifetime of the tube. The initial tube will be destroyed when one of the segments has visited $O(N)$ different contiguous sites. This requires a time $\tau_d \sim N^3/N_e$. In this time the chain has moved a distance comparable to its own size, therefore the diffusion constant D is expected to scale as N^{-2}. The theory predicts the following general power-law sequence

for the mean-square displacement in space, $g_1(t)$:

$$g_1(t) \sim \begin{cases} t^1, & t < \tau_0; \\ t^{1/2}, \tau_0 < t < \tau_e \sim N_e^2; \\ t^{1/4}, \tau_e < t < \tau_R \sim N^2; \\ t^{1/2}, \tau_R < t < \tau_d \sim N^3/N_e; \\ t^1, & t > \tau_d \end{cases} \tag{19}$$

which is shown schematically in Fig. (3). For the motion of the center-of-mass $g_3(t)$ one expects

$$g_3(t) \sim \begin{cases} t^1, & t < \tau_e \sim N_e^2; \\ t^{1/2}, \tau_e < t < \tau_R \sim N^2; \\ t^1, & \tau_R < t \end{cases} \tag{20}$$

These power laws are schematically indicated in Fig. 3 Direct experimental evidence for these intermediate time regimes has been seen NMR and diffusion of polymers at an interface, however simulations were the first to observe the crossover into the $t^{1/4}$ regime[3]. Indirectly the tube confinement is also seen by scattering experiments.

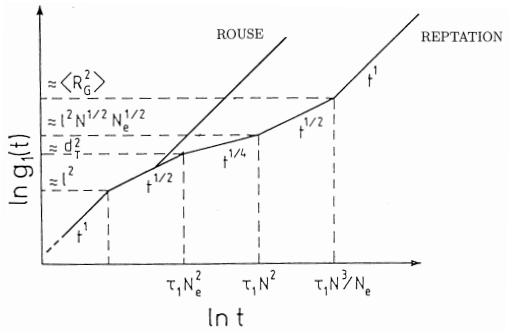

Figure 3. Schematic plot of the mean-square displacement for a monomer in the Rouse and the reptation model.

The reduced mobility also affects the relaxation of the long-wavelength modes $\mathbf{X}_p$. The relaxation time of mode p, with $N/p > N_e$ is enlarged by a factor of N/N_e, giving

$$\tau_{p,Rep} = \frac{N\langle R^2\rangle}{p^2}\frac{\zeta}{\pi^2 k_B T}\frac{N}{N_e} = \tau_R \cdot \frac{N^3}{3p^2} \sim \frac{N^3}{p^2} \tag{21}$$

The plateau modulus G_N^0 which was at the beginning when the similarities between melts and networks have been discussed, is determined from rheological experiments. Within the reptation model, it is related to the tube diameter $d_T = \langle R^2(N_e)\rangle^{1/2}$ and thus N_e via $G_N^0 = \frac{4}{5}\frac{\rho k_B T}{N_e}$. The prefactor 4/5 arises from tube length fluctuations, which allow for a somewhat more efficient relaxation under deformation, which is not the case for networks. The typical asymptotic properties are again summarized in the table:

	Rouse Regime $N < N_e, M < M_e$	Reptation Regime $N \gg N_e, M \gg M_e$
Diffusion	$D \propto N^{-1}$	$D \propto N^{-2}$
Relaxation Time	$\tau_R \propto N^2$	$\tau_d \propto N^3$
Viscosity	$\eta \propto N$	$\eta \propto N^3$
Modulus G_N^o ($t \ll \tau_d$)	$G_N^o = 0$	$G_N^o \propto \frac{kT}{N_e}$

It is one of the central current research topics on entangled polymer systems, how to determine N_e uniquely and how this actually quantitatively determines G_N^o. Before we go into that we discuss shortly the connection to classical network elasticity [1, 15, 30]. For this we go back to the random walk statistics of the chains and the idea of the Rouse model that an individual chain experiences all its surrounding only as a viscous background not affecting the conformations at all. For this we start with the probability distribution of chain ends:

$$P(\mathbf{R}) = \left(\frac{3}{2\sigma L \ell_K}\right)^{3/2} exp\left(-3R^2/2L\ell_K\right) \tag{22}$$

Since no specific inter-chain interactions are considered, $P(\mathbf{R})$ is the probability of a chain in a melt or a strand between two crosslinks in a network to be separated by a vector $\mathbf{R}$. The total number of possible conformations with a separation of $\mathbf{R}$ is the fraction $\Omega(\mathbf{R}) = \Omega_{tot} P(\mathbf{R})$ of all random walk conformations. This defines the entropy for a given $\mathbf{R}$ as

$$S = k_B \ell_K \Omega(\mathbf{R}) = const - 3k_B R^2/2L\ell_K \tag{23}$$

with the energy $U = 0$ (chain is viewed as a free random walk)

$$F = U - TS = \frac{3k_B R^2}{2L\ell_K} \tag{24}$$

for the conformation dependent contribution to the free energy of a chain with fixed end positions. This leads to an entropic force

$$\mathbf{f} = -\nabla F(\mathbf{R}) = -\frac{3k_B T}{L\ell_K}\mathbf{R} \tag{25}$$

the force of a linear elastic spring. The whole chain acts like a bond in the Rouse model. A random walk at a temperature T is a Hookean spring with spring constant $\sim T/N$. This almost trivial fact is the basis of all theories of network elasticity as well as a basis for the view of the Rouse chain to be a string of beads with linear elastic springs in between. No let us assume a perfect network with the crosslinks fixed in space. Under deformation $\underline{\underline{\lambda}}$ they move affinely with the macroscopic deformation of the box. Then the force contributed from each network strand is

$$\mathbf{f} = -\frac{3k_B T}{L\ell_K}\left(\underline{\underline{\lambda}} - \underline{\underline{1}}\right)\mathbf{R} \tag{26}$$

Each chain contributes with a force constant $\frac{3k_B T}{L\ell_K}$ to the restoring modulus of the system. Since there are ρ/N chains per unit volume present, we can use this to estimate

the stress in a given volume element of volume $V = B^3$. The probability that one chain cuts a plane with index $j(j = 1, 2, 3)$ is just R_j/B. The force component transmitted through this plane contributes from this subchain to $3k_BTR_iR_j/L\ell_KB^3$. Summing over all strands passing through our test volume and replacing R_iR_j by the ensemble average $\langle R_iR_j\rangle$ the microscopic stress tensor σ_{ij} reads

$$\sigma_{ij} = \frac{3k_BT\rho}{L\ell_KN}\langle R_iR_j\rangle \tag{27}$$

In analytic theory now usually a continuous path is taken for the chain and then taking the crossover to an infinitely small volume element, using $L = \ell \cdot N$ and for small N: $R_i/N \approx \partial R_i/\partial N$ one gets for the stress tensor

$$\sigma_{ij} = \frac{3k_BT\rho}{\ell\ell_K}\left\langle \frac{\partial R_i}{\partial n}\frac{\partial R_j}{\partial n}\right\rangle \tag{28}$$

Transforming from the bead index to the contour index s and taking the statistical segment length ($\ell\ell_K$) into account, this rewrites to

$$\sigma_{ij} = 3k_BT\frac{\rho}{N}\langle\frac{\partial r_i}{\partial s}\frac{\partial r_j}{\partial s}\rangle \tag{29}$$

for the microscopic formulation of the stress tensor in a polymer melt or network. In the affine picture this yields

$$G = k_BT\rho/N \tag{30}$$

In networks a variety of modifications are introduced. The above equation assumes an affine deformation of the whole system. This certainly is not the case! In an alternative approach the positions of the network beads at the box surface are fixed and the whole rest is only subject to connectivity constraints. In this phantom network model the modulus is somewhat reduced. In general, disregarding any entanglement contribution one can write

$$G = \frac{\rho kT}{N}[\nu - h\mu] \tag{31}$$

where ν is the number of active strands in a network (no closed loops ending in the same point, no free ends ...) and μ is the number of crosslinks. The quantity $0 \leq h \leq 1$ interpolates between the two models and is often taken as an adjustable parameter.

In the case of very long chains, $N \gg N_e$ so that the simple Rouse model assumption that the chains or strands act as non-interaction random walks a hierarchy of models trying to identify constraints has been introduced. They range from the constraint junction fluctuation approach of Flory all the way to the tube model. Ideas along these lines are employed to understand the spatial fluctuations in randomly crosslinked systems under strain. Taking all this one can view the strands in the Edwards tube as a continuation of entropic springs of length N_e, which leads to[15]

$$G_N^o = \frac{\rho k_BT}{N_e} \tag{32}$$

for networks and taking additional relaxation mechanisms into account

$$G_N^o = \frac{4}{5}\frac{\rho k_B T}{N_e} \tag{33}$$

for melts. This is the formula commonly used to determine N_e from measurements of the plateau modulus. A typical example in given in Fig. (4).

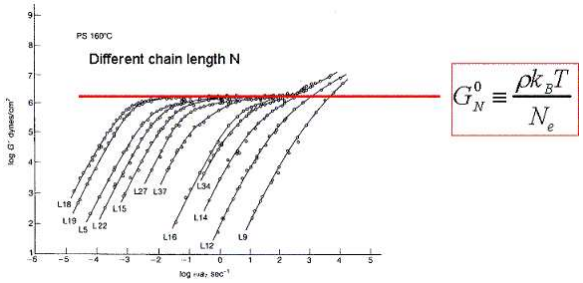

Figure 4. Experimental determination of the frequency dependent modulus $G'(\omega)$ of polystyrene melts for many different chain lengths, from[1]

Considering the previous discussion simulations nowadays do not focus that much any more on the question whether entanglements exist and whether they are relevant but more on their consequences and on the problem of how to quantify them properly. Typical topics are:

- Crossover to asymptotic power laws for η and D, what additional relaxation mechanisms exist and what kind of additional constraints, mechanisms might slow down the diffusion?
- How and why do different measurements of N_e give rather different results? Whatever are the links between different experimental observations?
- What are the effects of dilution and/or solvent quality in semidilute systems?
- What does the tube "look like"?
- Tube deformation and tube relaxation, quantitative and qualitative differences between networks and melts
- Swelling behavior with and without the influence of charges (polyelectrolyte gels).
- Polydispersity effects, mixtures as well as the influence of branched additives
- Structure property relations, can we predict N_e from the chemical structure of the polymer or any static measurement?

This list is not comprehensive, but it shows that the consensus that entanglements dominate many crucial properties is not really the end of a long development but rather defines many new research opportunities. To follow this by simulation we first have to describe how to prepare "good" initial states.

3.3 Simulation Models, Equilibrated Melts

Most of the following will be discussed for a freely jointed bead spring chain. The extension to other models is straight forward[10,31,5]. To study entanglement effects one can construct special model situations and study those. However more information applicable to experiment can be gained by studying "well equilibrated samples". A variety of methods to generate those has been discussed in other chapters. The most direct way would be to set up a system in an arbitrary state and equilibrate by running it for a few relaxation times. This however would need CPU time which by itself is of at least of the order of the running time of the whole project. Employing standard MD one typically can reach around $(2-4)\times 10^5$ particle steps per second on a single processor. A typical (large) time step is about $10^{-2}\ \tau$ for a dense Lennard Jones system (see below). For that system with $\tau_e \approx 2000\tau$ (estimated from the mean square displacement of inner beads, taking the stress relaxation after a step strain τ_e is estimated close to 10000 τ), one needs about $(2-5)\times 10^4$ steps or at least one second of CPU time per particle to reach τ_e[32]. Thinking of about $M = 100$ chains of $N \approx 800$, about $10N_e$, a system just big enough to compete with typical modern scattering experiments, for the fully flexible bead spring system defined below, we get $\tau_D \geq \tau_e \cdot (N/N_e)^3 = 10^3\tau_e$, equivalent to 10^3 sec per particle. Thus the above system on a single processor would require at least $M \cdot N \cdot 10^3 sec$, more than 20000 hours. Modern parallel systems reduce this time significantly, however, more complex models, such as semiflexible chains or models which more closely resemble the atomistic structure easily increase the time by several orders of magnitude time. For typical all atom models one can estimate the increase in CPU time roughly by the following. Taking about the same number of monomers for one entanglement molecular weight N_e (which is typically not enough) one can multiply the above time by the number of atoms per monomer (e. g. 4 for PE and 16 for PS ...) and the average ratio of the integration time steps, which is between 10^3 and 10^4. To reach the same relaxation, about 10^4 - 10^5 times more CPU time is needed, which is beyond reach. This estimate did not take into account the typically higher complexity of the force calculations! These numbers illustrate that the computers of the nearer future also will not solve the problem. Also, the tendency to reach high computing power by increasing the number of processors is not helpful since our systems are moderate in size but need long time runs. To study in very detail the final dependency of the elastic response of a system, one would need roughly 20 N_e and run that system for a time $\tau \gg \tau_e$ and eventually close to τ_d. Fortunately, for equilibration there are ways out. However, this requires a solid knowledge of the average equilibrium conformation[33]. In a melt or dense solutions the chains assume random walk statistics for all contour lengths $L \gg l_k$. Once a "sample" which reaches the asymptotic regime is available, one can use this as a reference state even for much longer chains. Values for internal distances, $\langle \Delta r_{ij}^2 \rangle$, have to fall on a general master curve. There are two typical options, internal distances or the chain form factor. For the internal distances $\langle \Delta r_{ij}^2 \rangle$ one finds

$$\langle \Delta r_{i-j}^2 \rangle \propto \begin{cases} \mid i-j \mid^2 & \mid i-j \mid \ell < \ell_k \\ \mid i-j \mid & \mid i-j \mid \ell \gg \ell_k \end{cases} \tag{34}$$

For distances $r \gg l$ beyond the local sphere or bead packing the crossover between the two regimes is approximated by the worm like chain model:

$$\langle \Delta r^2_{|i-j|=n} \rangle = nl^2 \left(\frac{1+\langle \cos\theta \rangle}{1-\langle \cos\theta \rangle} - \frac{1}{n} \frac{2\langle \cos\theta \rangle \left(1-\langle \cos\theta \rangle^n\right)}{\left(1-\langle \cos\theta \rangle\right)^2} \right) \tag{35}$$

where the asymptotic prefactor also is referred to as

$$c_\infty = \frac{1+\langle \cos\theta \rangle}{1-\langle \cos\theta \rangle}. \tag{36}$$

with $\langle \cos\theta \rangle$ the average bond angle "measured" between subsequent bonds. This function has to be determined in a complete simulation of shorter chains. Thus in a melt a system specific master plot gives $\langle \Delta r^2_{ij} \rangle / l \mid i-j \mid$ vs $l \mid i-j \mid$ the corresponding contour length. A characteristic example is given in Fig (5). This shows characteristic deviations from the theoretically expected curve for small distances, where the bead packing is dominant. For larger distances, the more flexible chains still show significant deviations. There the approximate formula of Eq. (5) is only useful as a general guide.

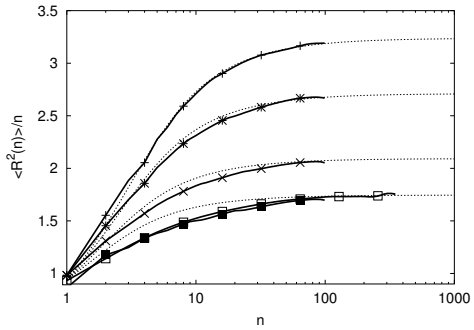

Figure 5. Normalized internal distances for different chain lengths for a standard bead spring LJ polymer, for different ℓ_K ranging from about $\ell_K = 1.7\sigma to 3.3\tau$. From[33]

In a similar way one can apply the analysis of the chain form factor $S(k)$

$$S(k) = \frac{1}{N} \left\langle \mid \sum_{j=1}^{N} e^{i\boldsymbol{k}\boldsymbol{r}_j} \mid^2 \right\rangle_{|k|} \tag{37}$$

where the index $\mid k \mid$ denotes a spherical average. In a melt one finds

$$S(k) \propto \begin{cases} N(1-\frac{1}{3}k^2\langle R_G^2\rangle) & \frac{2\pi}{k} \gg \langle R_G^2 \rangle \\ k^{-2} & \frac{2\pi}{\ell_k} \ll \frac{2\pi}{k} \ll \langle R_G^2 \rangle \\ k^{-1} & \frac{2\pi}{\ell} < \frac{2\pi}{k} < \frac{2\pi}{\ell_k} \\ O(1) & \frac{2\pi}{k} > \frac{2\pi}{\ell} \end{cases} \tag{38}$$

Besides the initial decay the form factor describes one characteristic, chain length independent curve. Fig. (6) shows a typical example.

Often the so-called Kratky plot, $k^2 S(k)$ vs k, is shown. Deviations from slope zero in the k^{-2} regime are easily to detect, even by eye. This helps for a quick check. Master plots of $S(k)$ or $\langle \Delta r^2_{ij} \rangle$ can be used to control the equilibration of melts.

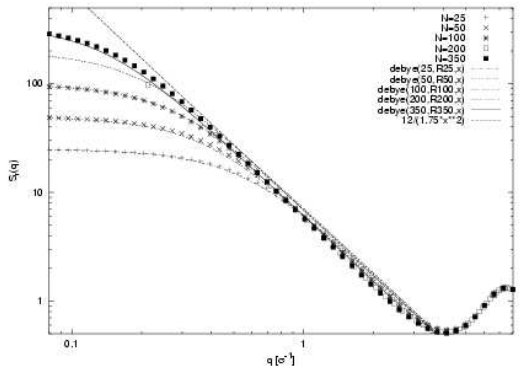

Figure 6. Chain form factor S(q) vs q for fully flexible LJ chains in a melt. Chain lengths range from N = 25 to N = 350. For fits the Debye function was used. The straight line indicates a slope of q^{-2}, from[34]

3.4 Preparing an Equilibrated Melt or Network, Specific Systems

A rather straight forward approach is to run a system by a reptation or slithering snake algorithm. This beats the slow realistic dynamics by a bit more than $O(N)$, however, is not really applicable for dense continuum systems. For semidilute solutions or lattice polymers at moderate densities and for moderate chain lengths this however is very appropriate. For dense continuum systems as well as systems with realistic chemical details such an approach fails. The strategy we meanwhile follow is as follows[33]:

- Simulate a melt of many short, but long enough chains ($N\ell \gg \ell_K$) into equilibrium by a conventional method
- Use this melt to construct the master curve or target function for the melts of longer chains (cf. Fig. (6))
- Create non reversal random walks of the correct bond length, which match the target function closely, especially at the longer distances. Introduce, if needed beyond the intrinsic stiffness of the bonds, stiffness via a suitable second neighbor excluded volume potential along the chain. (This might be a bit larger than the one of the full melt!)
- Place these chains as rigid objects in the system and move them around by a Monte Carlo procedure (shifting, rotating, inverting..., but **not** manipulating the conformation itself) to minimize density fluctuations
- Use this state as starting state for melt simulations
- Introduce slowly but not too slowly the excluded volume potential by keeping the short range interaction, taking care that in the beginning the chains can easily cross each other (see below)
- Run until the excluded volume potential is completely introduced. Control internal distances permanently to check for possible overshoots, deviations.
- Eventually support long range relaxation by so called end bridging[35,36] or double pivot moves

Independent on the details of the procedures, it is important to continuously compare the actual structure to the master or target curves. Ref.[33] also demonstrates some typical deviations from the master curve as they can occur during the set up.

As an example I now discuss the above steps along a recent publication[33] on simple bead spring chains[37,38]. An extension to other chains is straight forward. We consider bead with a unit mass. All beads interact via a purely repulsive LJ potential, to model the excluded volume interaction.

$$U_{LJ}^{r} = \begin{cases} 4\epsilon \left\{ (\sigma/r)^{12} - (\sigma/r)^{6} + \frac{1}{4} \right\} & r \leq r_c \\ 0 & r \geq r_c \end{cases} \tag{39}$$

with a cutoff $r_c = 2^{1/6}\sigma$. The beads are connected by a finite extensible non-linear elastic potential (FENE)

$$U_{FENE}^{(r)} = \begin{cases} -0.5 R_o^2 k \ell_n (1 - (r/R_o)^2) & r \leq R_o \\ \infty & r > R_o \end{cases} \tag{40}$$

in addition to the Lennard Jones Potential. The parameters are usually taken as $k = 30\epsilon/\sigma^2$, $R_o = 1.5\sigma$ in melt simulations. The temperature $T = \epsilon/k_B$ and the basic unit of time is $\tau = \sigma(m/\epsilon)^{1/2}$. Volume and temperature are kept constat and the bead density is $\rho = 0.85\sigma^{-3}$. The temperature was kept constant by coupling the motion to a Langevin thermostat. An alternative, which does not screen hydrodynamics is the DPD thermostat (cf. contribution by B. Dünweg). The average bond length with these parameters is $\langle \ell^2 \rangle^{1/2} = 0.97\sigma$. Chains of N beads each are considered.[b]

For this model in a melt of density $\rho = 0.85\sigma^{-3}$ the bond length is $\langle l^2 \rangle^{1/2} = 0.97\sigma$ with $c_\infty l^2 = ll_k = 1.7\sigma^2$. Since, in our case, there are no torsional barriers, the monomer packing relaxes quickly. It locally depends very sensitively on the ratio of bond length to effective excluded volume of the beads. Both do not allow **any** conclusion for the overall relaxation of the melt. The local packing only characterizes an equilibration on the smallest length scale considered and very small systematic deviations on that scale can lead to significant deviations from equilibrium at the large length scales on the order of the chain extension. For this system chains of $N = 350$ beads (which was not really needed in that case) were equilibrated by brute force simulations running in the background. Fig (5) also includes some data for stiffer chains. From these data we get the target function:

$$\langle R^2(\mid i-j \mid, N) \rangle / \mid i-j \mid \propto \ell \ell_k, \mid i-j \mid \ell \gg \ell_k \tag{41}$$

Having this reference state, we can proceed as mentioned before. The crucial steps are the last two. To introduce the exclude volume we proceed as follows:

1. Use a force-capped-Lennard-Jones-potential

2. increase the push-off time to make the procedure "quasi static".

[b] In addition a bending stiffness can be introduced via an effective three body interaction. With $cos\Theta_i = (\hat{\mathbf{r}}_{i,i-1} \cdot \hat{\mathbf{r}}_{i,i+1})$, with $\hat{\mathbf{r}}_{i,i-1} = (\mathbf{r}_i - \mathbf{r}_{i-1})/ \mid \mathbf{r}_i - \mathbf{r}_{i-1} \mid$ and accordingly $\hat{\mathbf{r}}_{i,i+1}$ the bending potential reads $U_{bend}(\Theta) = k_\Theta(1 - cos\Theta)$ By variation of k_Θ the model can be tuned from very flexible to very stiff.

The force capped potential we use reads :

$$\mathrm{U_{FCLJ}}(r) = \begin{cases} (r - r_{fc}) * \mathrm{U_{LJ}}'(r_{fc}) + \mathrm{U_{LJ}}(r_{fc}) & r < r_{fc} \\ \mathrm{U_{LJ}}(r) & r \geq r_{fc} \end{cases} \tag{42}$$

In the present case, r_{fc} is gradually reduced from the Lennard-Jones cut-off radius $r_c = 2^{1/6}\sigma$ to 0.8σ which is significantly smaller than the relevant interparticle distances, as illustrated in Fig. (7).

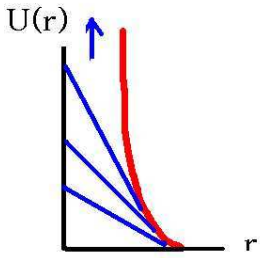

Figure 7. Illustration of the "force capped" Lennard Jones interaction used to introduce step by step the full excluded volume of the chains.

Force-capping has the advantage that this form of the soft potential systematically approaches the true potential. The typical time we used to introduce the full potential was about 50000τ, which is of the order of twice the Rouse time of a chain of N=100 beads. Such a procedure relatively safely equilibrates the internal conformations of the chains as Fig. (8) shows. There the results of a too fast and a proper push off procedure are shown for illustration. The too fast introduction shows the characteristic overshoot of the internal distances for small n. It is however also often rather important that the average end to end

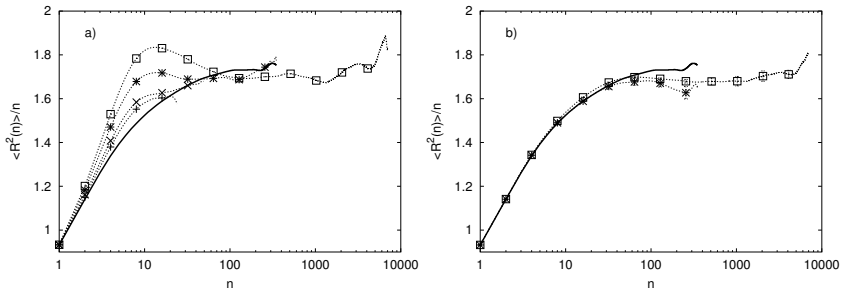

Figure 8. Mean square internal distances for chains of length N = 25 (+), 50 (x), 350 (*) and 7000 (□) for a too fast pushoff procedure (a) and the slower version as described in the text (b), from[33].

distance is close to the desired value, even though the overall number of chains might be relatively small. Then methods, which break and recombine chains, called the double-pivot or bridging algorithms are used. Note that they very effectively relax and manipulate large

distances, however affect small scales only extremely slowly! Having prepared melts by the above procedure we now can either perform standard simulations to study the melt or crosslink them in order to create networks by different methods.

The preparation of networks deserves another short comment.In the literature a number of different crosslinked systems has been studied extensively[34,39–43]. A typical range of systems in illustrated in Fig. (9)

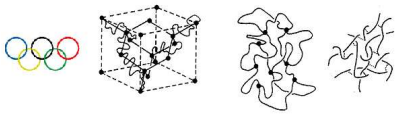

Figure 9. Typical crosslinked systems ranging from randomly crosslinked melts via various versions of endlinked polymer networks to the idealized lattice structure systems and the theorist's dream of an "olympic gel"

The randomly crosslinked system certainly is closer to experiments however encounters many difficulties[39]. Especially the dangling chain ends cause the relaxation to slow down dramatically (The time grows exponentially!), because it is linked to a retraction of the arms. Such effects are also known from other situations where branched polymers play an important role[2]. In addition the disorder or fluctuations are quenched. Thus simply running a system longer does not improve the data in comparison to experiment. For this one would need "many" medium sized systems or single extremely large ones. Thus we mostly stick to melts in the following.

3.5 Entanglement Analysis: Melts and Networks

In the following I will give a few examples of numerical experiments for melts and in some cases networks as well. The first almost trivial question is, whether the tube exists, the chain motion is confined and whether the noncrossability clearly makes a difference. Experimentally the determination of confinement is somewhat indirect and does not easily reveal the shape of the confining volume. Here simulations offer a unique way of visual inspection of the chain displacements. To do so one simply can plot the initial conformation of the chain and on top of that subsequent conformations. This is shown in Fig. (10) for network chains.

From other investigations we know that $35 < N_e$ and $100 > N_e$, which is nicely confirmed by the pictures. Depending on the view onto the initial conformation (the typical conformation of a random walk is a flattened thick cigar with a ratio of principal moments of inertia of $R_{11}^2 : R_{22}^2 : R_{33}^2 :\cong 11.8 : 2.5 : 1$) one clearly can identify the confinement. The diameter of the confining tube actually nicely fits results from earlier simulations on the mean square displacements. In a similar way one can also visualize the motion in polymer melts. There, however, due to a continuous release in the number of constraints, this for shorter chains, is more difficult to visualize. Thus one uses a small trick. What we now plot is not the bare conformation, but the back bone of the statically averaged chain contour, namely

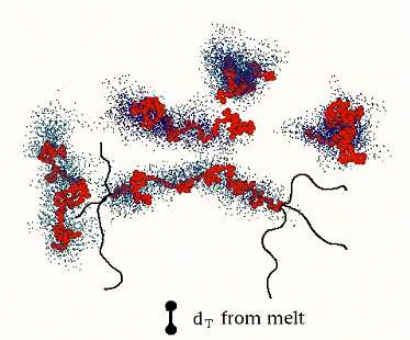

Figure 10. Time evaluation of the conformation of chains in an endlinked network of functionality $f = 4$,$N = 100$, where all network strands have the same length. The chains are, for clarity shown without the network. The indicated tube diameter was determined in an independent melt simulation, from[40].

$$\mathbf{R}_i = \frac{1}{n+1} \sum_{j=1-n/2}^{i+n/2} \mathbf{r}_i \tag{43}$$

This smoothens the contour and by a proper choice of n should be close to the back bone of the tube. Here $n = 35$ was used. These contours can then be plotted vs time and compared to a different system, where the chains can easily cross each other. For the full LJ interaction the barrier height is around $70kT$. One can introduce a potential, where the chains can cut through each other, but the pressure, $\langle R^2 \rangle$ and the bead friction ζ remain unchanged. These two systems are compared in Fig. (11) for chains of N = 350. While the confinement is not as easily visible as for the networks, the difference between the two

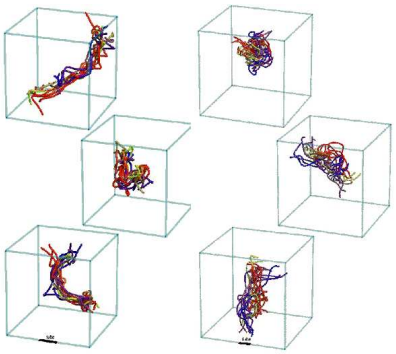

Figure 11. Time evolution of the coarse grained back bone of the chains for a melt of N = 350 bead chains for times up to the Rouse time τ_R. The left panel shows chains with the full excluded volume, while for the right panel the crossing barrier is only a few kT, from[34].

cases is striking, and nicely supports the tube idea.

Another direct test which shows the relevance of the noncrossability of the chains/network strands is shown in Fig. (12) For these networks with diamond lattice

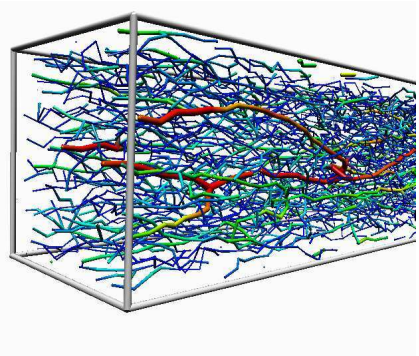

Figure 12. Elongated diamond lattice networks, where the only source of disorder are random links between network loops. The strands are colored due to their stretching (similar to the stress they carry) from small stretching (blue) to strong stretching (red). From[3]

connectivity were prepared. In order to fill space with the condition that the strands obey random walk statistics several interpenetrating networks are needed. This is the source of random linking of the different subnets. By this, "short topological paths" through the net are created, which under strong elongation carry most of the stress. Note that in this special example all "short chemical paths" have the same length.

After these intriguing pictures we can move to the data analysis which demonstrates the confinement not that directly, however is more closely related to possible experiments. The first to look at is the mean square displacement of the middle beads and the chains. Many studies on this have been performed[38,44–47], for an overview see[3] and computer simulations actually were the first to observe the slowing down of the motion clearly[38,48]. Fig. (13) shows results from a system of fully flexible polymers. More complicated models have

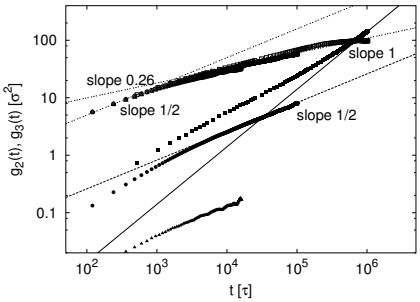

Figure 13. Mean square displacements $g_2(t)$ (open symbols) and $g_3(t)$ (closed symbols) for chain length $N = 350$ (□), 700 (○) and 10000 (△). The straight lines show power laws as guide to the eye. The local reptation power laws $g_2(t) \propto t^{1/4}$ and $g_3(t) \propto t^{1/2}$ are verified with remarkable clarity[32].

been studied by Faller and Müller-Plathe[49,50] and[45] for instance. Fig. (13) shows that the expected power laws are reproduced with a remarkable accuracy. From this a tube diameter of $7\sigma \leq d_T \leq 8\tau$ can be deduced, corresponding to an N_e of about $N_e \approx 30$, which is very small. To check the overall consistency the onset of the $t^{1/4}$ regime, the g_1, g_3 values at that time etc. are analyzed. In all cases the results roughly agree! Experiments also by now are able to analyse the chain motion directly and display the expected power laws. They however typically only cover a too small time window. To overcome this problem rather different temperatures are employed. It should however be noted that the shift in temperature not only affects the ratio k_BT/ζ but via conformational changes also N_e! Here simulations, despite of their many shortcomings are still superior.

Another important experimental technique is the neutron spin echo (NSE) method[27]. In NSE experiments the motion of the segments can be obtained by measuring the expectation value of the time-dependent single-chain structure function

$$S\left(\mathbf{k},t\right) = \frac{1}{N}\sum_{i,j}\left\langle \exp(i\mathbf{k}\cdot\left(\mathbf{r}_i(t)-\mathbf{r}_j(0)\right))\right\rangle . \tag{44}$$

For reptating chains deGennes calculated an expression for $S(k,t)$ neglecting the initial Rouse-like motion[51]. In recent simulations a slightly modified version is applied[52,53] which is identical to de Gennes result when a Gaussian model of the tube is explicitly assumed. We used this formula together with a correction for very long times (however, for the experimental NSE results or our present set of data this modification may be neglected):

$$\begin{aligned}\frac{S(k,t)}{S(k,0)} = &\left\{\left[1-\exp\left(-(kd/6)^2\right)\right]\cdot f\left(k^2b^2\sqrt{12Wt/\pi}\right)\right. \\ &\left.+\ \exp\left(-(kd/6)^2\right)\right\}\times\frac{8}{\pi^2}\sum_{p=1,odd}^{\infty}\frac{\exp\left(-tp^2/\tau_d\right)}{p^2},\end{aligned} \tag{45}$$

where $f(u) = \exp(u^2/36)\mathrm{erfc}(u/6)$. Note, that the derivation of deGennes does not take into account chain end effects and thus the above formula may only be applied in a narrow range of k-space $\frac{2\pi}{R_G} \lesssim k \lesssim \frac{2\pi}{d_T}$. Also since the initial Rouse-motion is not explicitly described, this formula only applies for $t > \tau_e$ (The short time motion only enters through the inverse friction coefficient $W = k^T/\zeta\ell\ell_K$).

What one finds there is a rather strong dependency of chain length N or the value of d_T deduced from the plot. Even for $N = 10000$ one finds N_e significantly larger than the result from the mean square displacements. Though these are, to my knowledge, the best data available, there might be some problems with the statistics (N = 10000). Note that for these data the conformations of the longest chains were not prepared by the procedure discussed before, while all the shorter chains simply ran long enough!

The standard experimental method to determine $N_{e,p}$ (for clarity we index N_e determined from the plateau-modules with an additional index p) is by measuring the plateau modulus under oscillatory shear[15,1]. Alternatively, it is also possible to measure the normal stress decay $\sigma_N(t)$ in a step strain elongation. Since the latter is much simpler to perform in a simulation, volume conserving step strain runs were performed for four different amplitudes $\lambda = 1.25$, 1.5, 1.75 and 2.0. The normal stress was σ_N was determined by the

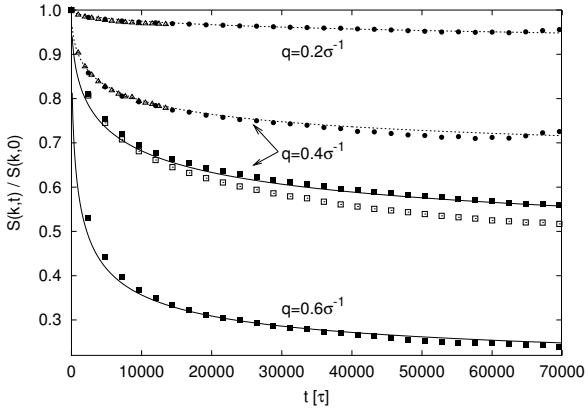

Figure 14. $S(k,t)$ for different chain lengths: $N = 10000(\triangle)$, $N = 2000(.)$, and $N = 700(\square)$ and the centered subchain of length 550 of the same $N = 700$ chains ($\blacksquare$). Continuous curves are simultaneous fits to the $N = 2000$ data corresponding to $d_T = 9.6\sigma$. The dotted curve is a simultaneous fit to the N = 700, 550 monomer subchain with a tube diameter of $d_t = 12.9\sigma$.[32,54]

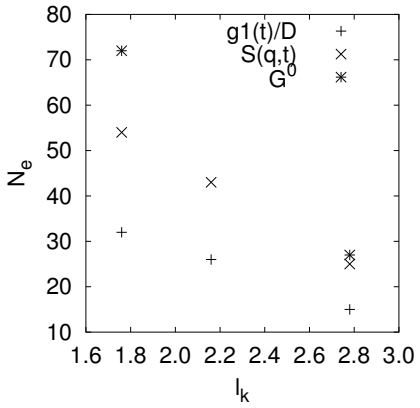

Figure 15. N_e as a function of the Kuhn length of the chains ℓ_k determined from the mean square displacements, the scattering function and the modulus.

microscopic virial-tensor. The plateau-values of the stress were fitted to the stress-strain formulas for classical rubber elasticity (CRE)[55] $\sigma_N = G\left(\lambda^2 - \frac{1}{\lambda}\right)$ and to the Mooney-Rivlin (MR) formula[56] $\sigma_N = 2G_1\left(\lambda^2 - \frac{1}{\lambda}\right) + 2G_2\left(\lambda - \frac{1}{\lambda^2}\right)$ to determine G_N^0. MR gives $G_N^0 = 0.0105 k_B T \sigma^{-3}$ while CRE gives $G_N^0 = 0.008 k_B T \sigma^{-3}$. It is known experimentally that MR slightly overestimates the modulus while CRE always underestimates it. The standard formula[1] to calculate $N_{e,p}$,

$$G_N^0 = \frac{4}{5}\frac{\rho k_B T}{N_{e,p}}, \tag{46}$$

gives $N_{e,p} \approx 65$ for the MR fit and $N_{e,p} \approx 80$ for the classical formula. Both values

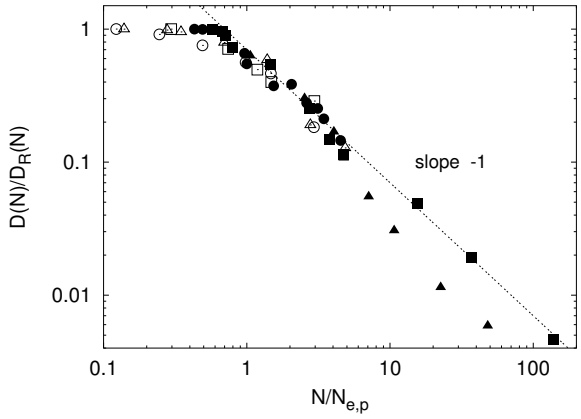

Figure 16. Scaled diffusion constant $D(N)/D_R(N)$ vs. scaled chain length $N/N_{e,p}$ for polystyrene (•) ($M_{e,p} = 14600$, $T = 485K$), polyethylene (■) ($M_{e,p} = 870$, $T = 448K$), PEB2 (▲) ($M_{e,p} = 990$, $T = 448K$), the present bead spring model (△) ($N_{e,p} = 72$), the bond-fluctuation model for $\Phi = 0.5$ (□) ($N_e = 30$) and tangent hard spheres at $\Phi = 0.45$ (○) ($N_e = 29$). All data are scaled with $N_{e,p}$ from the plateau modulus or with $2.25N_e$ from $g_1(t)$. From[32]

are much higher than our previous estimate, $N_e = 32$. From a theoretical point of view this discrepancy might not be relevant, since the prefactors in the reptation model are not rigorously determined. For practical issues, however, like comparing results from various experiments and simulations the difference is relevant.

At this point we can conclude that we are able to clearly observe and demonstrate entanglement effects. However the different values originating from different experiments prohibit to give an overall consistent picture. Fig. (15) shows the outcome of such investigations as we plot the entanglement molecular weight as a function of stiffness for different "experimental" tests. This illustrates that one has to decide on one definition of N_e. Taking the original discussion on the chain confinements, the results taken from the modulus be taken as a reference state. If done like this, one can use this to scale other measurements. Fig. (15) shows the scaled diffusion constants for a variety of experiments. The actual diffusion constant $D(N)$ is normalized by the hypothetical Rouse regime diffusion constant $D_R(n)$ as it can be extrapolated from short chain simulations or experiments. However, ut should be noted that a similar plot employing e. g. S(k, t) will lead to different fits for N_e for different polymers or models systems.

3.6 Structure and Property Relations

Though a general picture emerges, there is still the problem of the structure property relation. Is there a way to predict N_e or at least one value for a specific experiment based on the conformations, meaning the chemistry alone?

We saw that with increasing stiffness, the value of N_e decreased, however, the ratio of the different values obtained from the mean square displacements, scattering and modulus did not remain constant. Also, the modulus always predicted the largest value. This seems to hold for simple bead spring chains, while there are chemical systems where this is not

the case. Polycarbonate as an example of a technically very important polymer (e. g. for compact discs) has an $N_e \approx 6$ from the modulus, while the mean square displacement suggests via a scaling from Fig. (15) a value of $N_e \approx 12$[57]. Obtaining just one measurement obviously is not sufficient! Thus there is a significant need for a predictive theory or ansatz, which determines a value of N_e from the chain conformations, which then can be used to predict the other quantities, especially the modulus. How different N_e, or M_e respectively is shown in the table. A typical ambient temperatures (note that the M_e depends on temperature just as the overall chain extension does) one obtains the following values:

	PE (Polyethylene)	PS (Polystyrene)	PDMS (Polydimethyl-Siloxane)	BPA PC (Polycarbonate)
N_e	100	170	135	5 - 7
M_e	1400	18000	10000	≈1700

Even within one class of materials significant differences can be observed, as indicated in Fig (17). There different modifications of polycarbonate are shown, which within experimental accuracy have about the same Kuhn length ℓ_K but rather different entanglement lengths, as indicated[58,59].

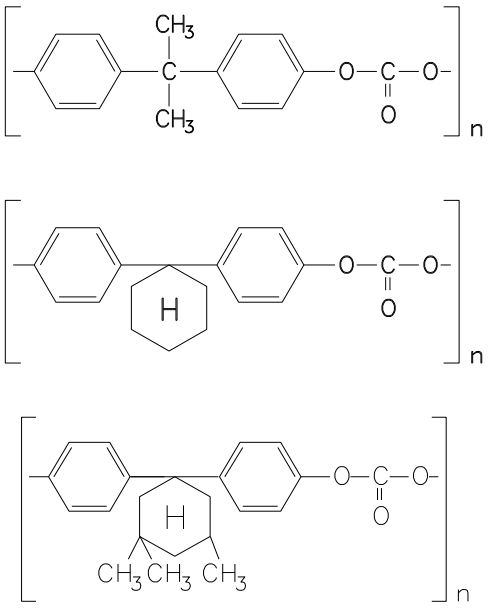

Figure 17. Structure of different polycarbonate modifications, the respective entanglement molecular weight are $N_e \approx 6, 10, 15$ from top to bottom.

These results demonstrate a key problem for a successful link between the more basic science, generic phenomena, oriented research and modern materials science. Our understanding has to become more quantitative. This holds for many fields in the science of microscopically or nanoscopically designed molecular structures as well as for more conventional bulk systems. Because of the huge relaxation times a factor of 2 in the entanglements change the viscosity also by a factor of $2^{1.4} \approx 2.6$ and similar reduces the

diffusion constant. Uncertainties of this order in predictions are relatively small, however, are of significant experimental and technological relevance.

Is there a way to understand these deviations as well as the sensitivity to chemical structure and conformation? Over the years several criteria have been developed to identify entanglements. One set of publications deals with an analysis of the topological structure of a network and related approximations for melts[60]. For this the problem however is that multi chain / multi ring effects can in all cases (Gauss integrals, Alexander polynominals ...) can only be taken into account up to a finite order. How important many chain effects can be is illustrated by Fig. (18) for an example of three chains only[42,61].

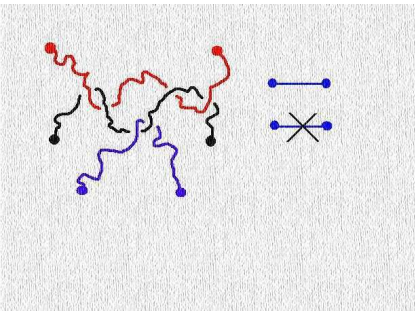

Figure 18. Constraints between two chains (red, black) depend on the presence of the 3rd chain.

In principle one would need for long chains an "infinite" hierarchy of such interactions. On the other hand, in order to observe N_e is dependent on N for $N \gg N_e$ a constant average density of constraints along the back bone of the chain is needed to provide the tube. Iwata and Edwards[61,62] tried to overcome this by looking at the local values of the Gauss integral upon numerical integral. All this suggests that the local chain-chain packing plays a crucial role. Therefor relatively early first attempts were made to relate N_e to the number of different cains within the value d_T^3[63,64]. All these attempts were not really satisfactory. More recently a collection of many moduli data of different polymers Fetters et al[18,19] suggest that the modulus is related to the so called chain packing length $p = N/\rho\langle R\rangle$, which is a good measure for the spatial packing, in a way that $G \sim p^{-3}$. Many polymers seem to follow that within a $\pm 20\%$ corridor. This however still does not explain how this packing is able to produce the entanglement mesh. Beyond that Everaers et al.[20] just recently performed a topological analysis of a number of different polymer melts and dense solutions. They studied simple bead spring chains of different stiffness as well as simplified model for polycarbonate. In all cases the data of G_N^0 derived from the topological determination of the primitive path and the analysis from analyzing normal stress differences after a step strain quantitatively agree. Thus it seems that (1) there is a way to relate purely static quantities to the modulus with reasonable accuracy and (2) the tube model can quantitatively be linked to a topological analysis of the state of the melt. With this we arrive at the question of the very beginning, namely to what extent does the fact that the chains do not pass through each other, influence the relaxational properties of these fascinating ultra soft solids or viscoelastic liquids. Based on recent

progress in various fields extensions to more complicated systems such as mixtures of linear and branched polymers or more stiff polymers, as they can be found in biological systems, are underway.

4 Summary

In the first part of this contribution certain aspects concerning the dynamics and stress relaxation in polymer melts or networks, complementary to the other contributions has been discussed. In addition typical "measurements" to study reptating polymer melts have been mentioned. From this a basic ingredient to study the dynamics of polymer melts and networks, namely the equilibration and preparation of suitable starting conformations has been presented in more detail. This is a crucial condition for the next step, namely to study both the dynamic development as well as the conformational properties of a system. Then a few typical examples of numerical tests performed over the last years illustrated, what can be done by simulations and dense model systems employing modern numerical methods and computers.

Acknowledgement

I would like to thank many collaborators over many years of research. The topics described above benefitted especially from longstanding fruitful interaction with G. S. Grest and R. Everaers.

References

1. M. Doi and S. F. Edwards. *The Theory of Polymer Dynamics*. Clarendon, Oxford, 1986.
2. T. C. B McLeish. Tube theory of entangled polymer dynamics. *Adv. in Phys.*, 5:1379 1527, 2002.
3. K. Kremer and G. S. Grest. In K. Binder, editor, *Monte Carlo and Molecular Dynamics Simulations in Polymer Science*, page 194. Oxford University Press, New York, 1995.
4. C. F. Abrams and K. Kremer. *J. Chem. Phys.*, 116:3162, 2002.
5. K. Kremer. *Soft and Fragile Matter, Nonequilibrium Dynamics, Metastability and Flow*. NATO ASI Workshop, St. Andrews, 2000.
6. K.Kremer C. F. Abrams, L. DelleSite. In M. Mareschal and G. Ciccotti, editors, *Bridging Time Scales: Molecular Simulations for the Next Decade*. Springer, Berlin, Heidelberg, 2002.
7. P. G. de Gennes. *Scaling Concepts in Polymer Physics*. Cornell University Press, Ithaca NY, 1979.
8. M. Rubinstein and R. Colby. *Polymer Physics*. Oxford, Oxford, 2003.
9. A. R. Khokhlov A. Yu Grosberg. *Statistical Physics of Macromolecules*. AIP Press, New York, 1994.
10. K. Binder. In K. Binder, editor, *Monte Carlo and Molecular Dynamics Simulations in Polymer Science*, page 356. Oxford University Press, New York, 1995.

11. P. E. Rouse. *J. Chem. Phys.*, 21:1272, 1953.
12. F. Bueche. *J. Chem. Phys.*, 22:603, 1954.
13. W. Paul, G. D. Smith, D. Y. Yoon, B. Farago, S. Rathgeber, A. Zirkel, L. Willner, and D. Richter. Chain motion in an unentangled polyethylene melt: A critical test of the rouse model by md simulatons and neutron spin echo spectroscopy. *Phys. Rev. Lett.*, 80:2346, 1998.
14. H. Tao, T. P. Lodge, and E. D. von Meerwall. *Macromolecules*, 33:1747, 2000.
15. J. D. Ferry. *Viscoelastic Properties of Polymers*. Wiley, New York, 1980.
16. S. F. Edwards. *Proc. Phys. Soc.*, 92:9, 1967.
17. P. G. de Gennes. *J. Chem. Phys.*, 55:572, 1971.
18. L. J. Fetters, D. J. Lohse, S. T. Milner, and W. W. Graessley. *Macromolecules*, 32:6847, 1999.
19. L. J. Fetters, D. J. Lohse, and W. W. Graessley. *J. Pol. Sc. B. Pol. Phys.*, 37:1023, 1999.
20. R. Everaers, S. K. Sukumaran, G. S. Grest, C. Svaneborg, A. Sivasubramanian, and K. Kremer. *preprint*, 2003.
21. S. T. Milner and T. C. B. McLeish. Star polymers and failure of time-temperature superposition. *Macromolecules*, 31:8623, 1998.
22. G. S. Grest, M. Pütz, R. Everaers, and K. Kremer. *J. Non-Crystal. Solids*, 274:139, 2000.
23. B. Mergell and R. Everaers. *Macromolecules*, 34:5675, 2001.
24. P. Flory. *Principles of Polymer Chemistry*. Cornell University Press, Ithaca, 1953.
25. G. Fleischer and F. Fujara. In R. Koesfeld and B. Blümich, editors, *NMR Basic Principles and Progress*. Springer-Verlag, Heidelberg, 1994.
26. H. W. Spiess. *Macromol. Symp.*, 174:111, 2001.
27. B. Ewen and D. Richter. *Adv. Pol. Sci.*, 134:3, 1997.
28. D. S. Pearson. *Rubber Chem. Tech.*, 60:439, 1987.
29. D. S. Pearson, L. J. Fetters, W. W. Graessley, G. ver Strate, and E. von Meerwall. *Macromolecules*, 27:711, 1994.
30. S. F. Edwards and T. A. Vilgis. *Rep. Prog. Phys.*, 51:243, 1988.
31. K. Kremer. *Computer simulation methods for polymer physics*. Iatl. Phys. Soc., Rome, 1996.
32. M. Pütz, K. Kremer, and G. S. Grest. *Europhys. Lett.*, 49:735, 2000.
33. R. Auhl, R. Everaers, G. S. Grest, K. Kremer, and S. J. Plimpton. *J. Chem. Phys.*, 2003.
34. M. Pütz, *Dynamik von Polymerschmelzen und Quellverhalten ungeordneter Netzwerke*, Ph.D. Thesis, University of Mainz, 1999.
35. V. G. Mavrantzas, T. D. Boone, E. Zervopoulou, and D. N. Theodorou. *Macromolecules*, 32:5072, 1999.
36. A. Uhlherr, S. J. Leak, N. E. Adam, P. E. Nyberg, M. Doastakis, V. G. Mavrantzas, and D. N. Theordorou. Large scale atomistic polymer simulations using Monte Carlo methods for parallel vector processors. *Comp. Phys. Comm.*, 144:1, 2002.
37. G. S. Grest and K. Kremer. *Phys. Rev. A*, 33:3628, 1986.
38. K. Kremer and G. S. Grest. *J. Chem. Phys.*, 92:5057, 1990.
39. E. R. Duering, K. Kremer, and G. S. Grest. *Phys. Rev. Lett.*, 67:3531, 1991.
40. E. R. Duering, K. Kremer, and G. S. Grest. *J. Chem. Phys.*, 101:8169, 1994.

41. M. Pütz, R. Everaers, and K. Kremer. Self-similar chain conformations in polymer gels. *Phys. Rev. Lett.*, 84:298, 2000.
42. R. Everaers and K. Kremer. *Phys. Rev. E*, 53:R37, 1996.
43. R. Everaers. *New J. Phys.*, 1:12.1, 1999.
44. W. Paul, K. Binder, D. W. Heermann, and K. Kremer. *J. Chem. Phys.*, 95:7726, 1991.
45. W. Paul, K. Binder, K. Kremer, and D. W. Heermann. *Macromolecules*, 24:6323, 1991.
46. S. W. Smith, C. K. Hall, and B. D. Freeman. *J. Chem. Phys.*, 104:5616, 1996.
47. M. Kröger and H. Voigt. On a quantity descrbing the degree of entanglement in linear polymer systems. *Macromol. Theory Simul.*, 3:639, 1994.
48. K. Kremer, G. S. Grest, and I. Carmesin. *Phys. Rev. Lett.*, 61:566, 1988.
49. R. Faller, F. Müller-Plathe, and A. Heuer. *Macromolecules*, 33:6602, 2000.
50. R. Faller and F. Müller-Plathe. *Chem. Phys. Chem*, 2:180, 2001.
51. P. G. de Gennes. *J. Phys. (Paris)*, 42:735, 1981.
52. K. Kremer and K. Binder. *J. Chem. Phys.*, 81:6381, 1984.
53. M. Doi. *J. Phys. A*, 8:959, 1988.
54. M. Pütz, K. Kremer, and G. S. Grest. *Europhys. Lett.*, 52:721, 2000.
55. L. R. G. Treloar. *The Physics of Rubber Elasticity*. Clarendon Press, Oxford, 1986.
56. M. Mooney. *J. Appl. Phys.*, 11:582, 1940.
57. S. Leon and K. Kremer. *in preparation*.
58. K. Sommer, J. Batoulis, W. Jilge, L. Morbitzer, B. Pittel, R. Plaetschke, K. Reuter, R. Timmermann, K. Binder, W. Paul, F. T. Gentile, D. W. Heermann, K. Kremer, M. Laso, U. W. Suter, and P. J. Ludivice. Correlation between primary chemical structure and property phenomena in polycondensates. *Advanced Materials*, 3:590, 1991.
59. J. Baschnagel, K. Binder, P. Doruker, A. A. Gusev, O. Hahn, K. Kremer, W. L. Mattice, F. Müller-Plathe, M. Murat, W. Paul, S. Santos, U. W. Suter, and V. Tries. *Advances in Polymer Science: Viscoelasticity, Atomistic Models, Statistical Chemistry*. Springer Verlag, Heidelberg, 2000.
60. W. Michalke, M. Lang, S. Kretmeier, and D. Gönitz. *Phys. Rev. E*, 64:012801, 2001.
61. K. Iwata and S. F. Edwards. *J. Chem. Phys.*, 90:4567, 1989.
62. K. Iwata. *Macromolecules*, 24:1107, 1991.
63. T. A. Kavassalis and J. Noolandi. *Phys. Rev. Lett.*, 59:2674, 1987.
64. T. A. Kavassalis and J. Noolandi. *Macromolecules*, 22:2709, 1989.